



An Electrochemical and XRD Study of Lithium Insertion into Mechanically Alloyed Magnesium Stannide

G. A. Roberts,^{a,*} E. J. Cairns,^{**} and J. A. Reimer

Environmental Energy Technologies Division, Ernest Orlando Lawrence Berkeley Laboratory, and Department of Chemical Engineering, University of California at Berkeley, Berkeley, California 94720, USA

The intermetallic Mg_2Sn is a promising negative electrode material for rechargeable lithium cells. Preliminary cycling tests have demonstrated stable capacities at 400 mAh/g for 20 cycles. Magnesium stannide was produced by mechanically alloying magnesium and tin powders. Mechanical alloying can convert the equilibrium Mg_2Sn phase to a metastable phase by the introduction of defects with extended milling times. *In situ* X-ray diffraction has shown that the cubic Li_2MgSn phase, which is similar in size and structure to cubic Mg_2Sn , is produced by lithium insertion into the equilibrium and metastable phases. The conversion from the metastable phase is irreversible, so subsequent lithium removal from Li_2MgSn produces the equilibrium Mg_2Sn phase.
© 2003 The Electrochemical Society. [DOI: 10.1149/1.1578477] All rights reserved.

Manuscript submitted October 24, 2002; revised manuscript received January 30, 2003. Available electronically May 16, 2003.

Several intermetallics, such as Cu_6Sn_5 and $InSb$, have been investigated as possible replacements for graphite negative electrodes in rechargeable lithium batteries.¹⁻⁴ While these are promising materials with higher maximum capacities than graphite, adequate cycling stability has only been demonstrated with cycling conditions that limit the capacities to well under 300 mAh/g. Therefore, improving these known intermetallic hosts and identifying new intermetallics capable of storing lithium are active research topics.

We have studied the only intermetallic in the Mg-Sn system, magnesium stannide. Mg and Sn are abundant and inexpensive materials that can serve as lithium hosts at room temperature. In this study, we have examined the mechanical alloying synthesis of Mg_2Sn , the behavior of Mg_2Sn during galvanostatic cycling, and the structural changes that occur during lithium insertion by *in situ* X-ray diffraction (XRD). We note that Mg_2Sn is structurally similar to Mg_2Si , which has been the focus of studies in our group and others.⁵⁻⁹

Mg_2Sn can be transformed from the equilibrium cubic structure to a metallic high pressure phase. The nature of this metastable phase is still being debated. Cannon and Conlin produced it at temperatures over 400°C and pressures over 25,000 bar.¹⁰ Dyuzheva *et al.* successfully preserved the high pressure phase at ambient conditions and classified it as a hexagonal Mg_2Sn polymorph.¹¹ Range *et al.* concluded that it crystallized trigonally and argued that the phase may actually have a composition of Mg_3Sn_5 .¹² The metastable phase has also been produced by mechanical alloying. Schilz *et al.* noted its formation while milling a ternary Mg-Si-Sn blend.¹³ Clark *et al.* produced a mixture of the phases and tentatively classified the metastable phase as orthorhombic.¹⁴ Finally, Urretavizcaya and Meyer classified the milled metastable phase as hexagonal.¹⁵

Electrochemical cycling results have been published for the cubic phase, the metastable phase, and a combination of the phases.¹⁶ The results indicated that a mixture of the cubic and metastable phases cycled best with reversible capacities of approximately 350 mAh/g. The authors proposed a cooperative effect between the phases with the metastable phase supplying most of the capacity and with the cubic phase relieving stresses from lithium insertion and removal.

In another study, a mechanism was proposed for lithium insertion in a mixture of the two Mg_2Sn phases.¹⁷ The authors concluded that lithium intercalates into Mg_2Sn and that Li-Sn alloys are formed after the intercalation limit is reached. This mechanism is similar to

their proposed mechanism for lithium insertion into Mg_2Si , with the exception that they proposed Li-Mg reactions for Mg_2Si but not for Mg_2Sn .⁸

This proposed mechanism has a few issues that need to be resolved. For example, the Mg_2Sn differential capacity plots only developed strong peaks characteristic of Li-Sn reactions after several cycles.¹⁷ Since the initial capacities were as large as 450 mAh/g, which corresponds to approximately 2.8 lithium atoms per Mg_2Sn unit, another mechanism besides intercalation is probably required to accommodate the large amount of inserted lithium. Also, they reported that they were only able to produce a mixture of the two Mg_2Sn phases by milling. In this study, we have prepared each phase individually and studied the cycling behavior of the materials by galvanostatic cycling and *in situ* XRD.

Experimental

Mg_2Sn was synthesized by ballmilling Mg (99.8% purity, -325 mesh, Alfa Aesar) and Sn (99.85% purity, 100 mesh, Alfa Aesar) powders in a planetary ball mill (Fritsch Pulverisette 6 Mono-Mill). The 316 stainless steel (SS) milling vessel has a cavity volume of 45 mL and can be sealed with an O-ring. Ten grams of powder, fifteen balls (316 SS, 3/8 in. diam), and a few mL of hexane were added to the milling vessel in an argon-filled glove box. A mill setting of 400 rpm was used for all of the experiments.

Electrode slurries were prepared by mixing 80 wt% Mg_2Sn , 10 wt% polyvinylidene fluoride PVDF, dissolved in *n*-methyl-2-pyrrolidinone, and 10 wt% acetylene black. The slurry was spread evenly on copper foil with 10 mil shims. The slurry was dried under vacuum at 120°C. After drying, 5/8 in. diam electrodes were punched from the copper foil. This procedure produced electrodes with approximately 15 mg of active material.

Galvanostatic cycling experiments were performed with Arbin battery cyclers in the SS cells shown in Fig. 1. The cells were assembled with lithium foil counter electrodes, Celgard 3401 separators, and Merck Selectipur LP-40 electrolyte (1 M $LiPF_6$ in 1:1 diethyl carbonate:ethylene carbonate). Unless otherwise noted, the cells were cycled over 5-900 mV vs. Li/Li^+ at current densities of 50 mA/g active material. The cells were held at open circuit for 0.5 h at the end of each charge and discharge step. The capacities are reported with respect to the mass of the Mg_2Sn powder only.

The electrochemical cell used for reflection-mode *in situ* XRD measurements was constructed from stainless steel with a beryllium window and an O-ring seal. This cell is described in detail in another manuscript.⁵

Ex situ XRD was performed on a Siemens Diffraktometer D5000 ($Cu K\alpha$). *In situ* XRD was performed on a Rigaku diffractometer ($Cu K\alpha$) with an Inel CPS-120 position-sensitive detector. The *in situ* diffraction patterns were signal-averaged for 15 min.

* Electrochemical Society Student Member.

** Electrochemical Society Fellow.

^a Present address: Sandia National Laboratories, Analytical Materials Science Department, Livermore, CA 94550.

^z E-mail: garober@sandia.gov

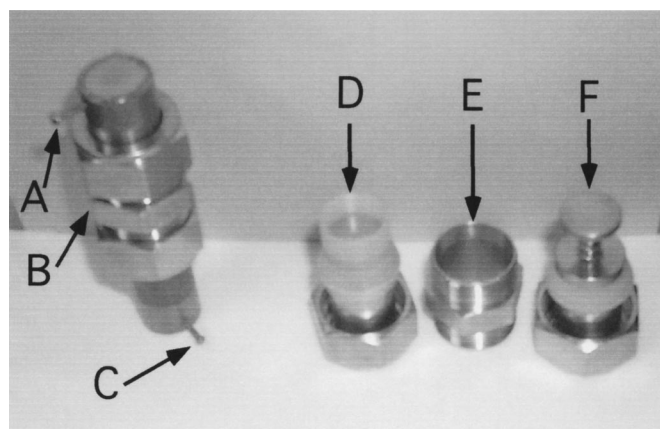


Figure 1. Photograph of assembled and unassembled cells: (a) counter electrode terminal; (b) reference terminal; (c) working electrode terminal; (d) working electrode assembly; (e) union; (f) counter electrode assembly.

Results and Discussion

Mg₂Sn synthesis.—XRD patterns of powder samples removed during the mechanical alloying synthesis are shown in Fig. 2. After 3 h of milling, the cubic Mg₂Sn phase was the most abundant. The metastable phase was observed after 6 h of milling, and it was the only phase detected after 20 h of milling. The cubic phase could be recovered by annealing the metastable phase at 350°C for several hours. Figure 3 shows the XRD pattern of the metastable phase with the indexed JCPDS pattern for a hexagonal Mg₂Sn phase with space group *P6₃/m* (pattern number 33-0866). This indexed pattern fits our experimental data as well as any of the other proposed structures for this complex phase, so we refer to the metastable phase as h-Mg₂Sn and to the cubic phase as c-Mg₂Sn throughout this paper.

Figure 4 shows the powder composition vs. milling time for a milling batch. The compositions of each sample were calculated from the relative XRD peak intensities of each phase. The c-Mg₂Sn structure formed rapidly during milling. The h-Mg₂Sn phase was produced by conversion of the c-Mg₂Sn phase instead of by direct synthesis from the elemental powders. The cubic to hexagonal conversion was completed after 20 h of milling.

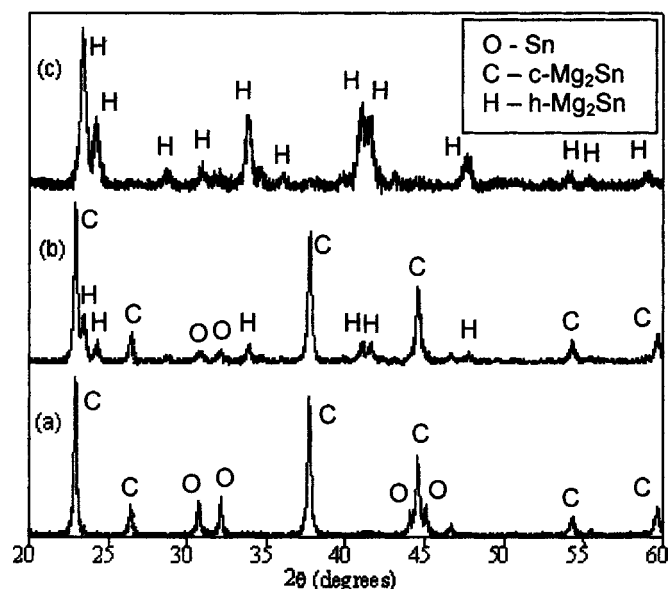


Figure 2. XRD patterns during synthesis: (a) 3 h; (b) 6 h; (c) 20 h.

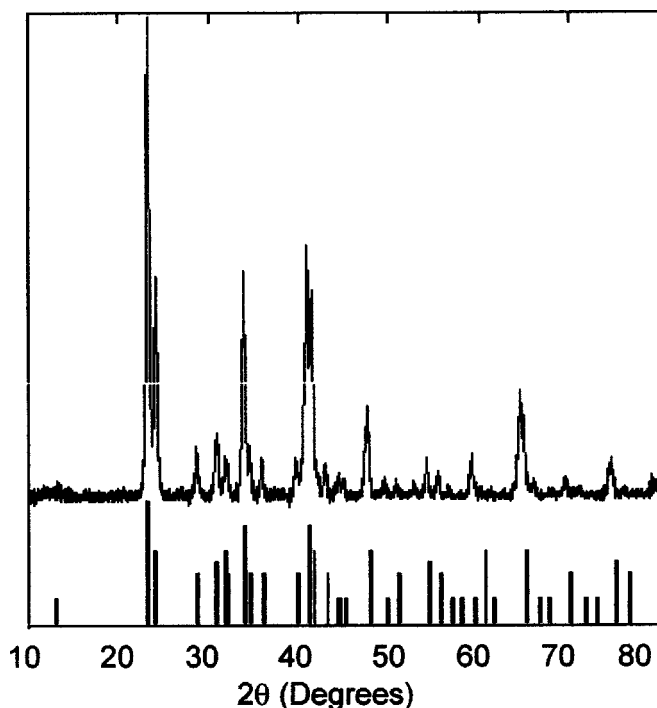


Figure 3. Experimental and indexed XRD patterns for h-Mg₂Sn.

Producing a metastable crystalline phase by milling an equilibrium phase is unusual. Metastable solid solutions and amorphous phases are often produced by milling, but they are generally produced by kinetic limitations. The atomic mobilities of the components are normally too low at the milling temperatures to permit atomic rearrangements to form equilibrium structures.¹⁸ However, in this case, the metastable phase is produced only after the equilibrium phase is formed, so there must be a thermodynamic driving force that leads to the formation of the metastable phase. A possible explanation is that the defects introduced by high energy milling can effectively raise the free energy of the equilibrium phase above the free energy of the metastable crystalline phase. Such effects have been estimated to be capable of driving phases as far as 30 kJ/mol from equilibrium in other systems.¹⁸

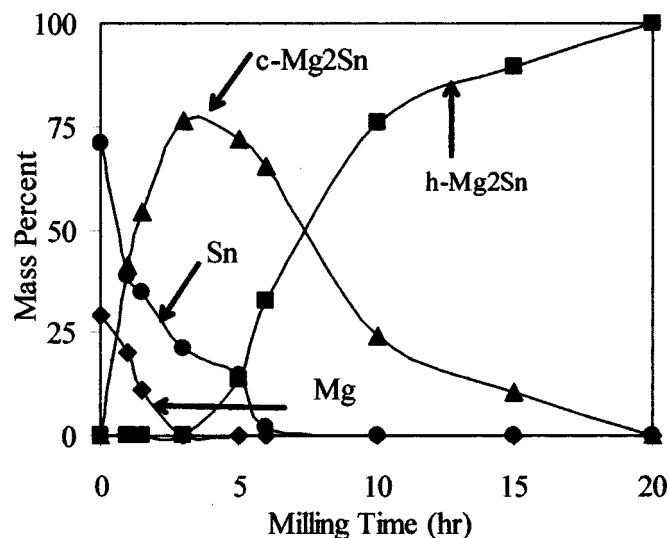


Figure 4. Powder composition vs. milling time.

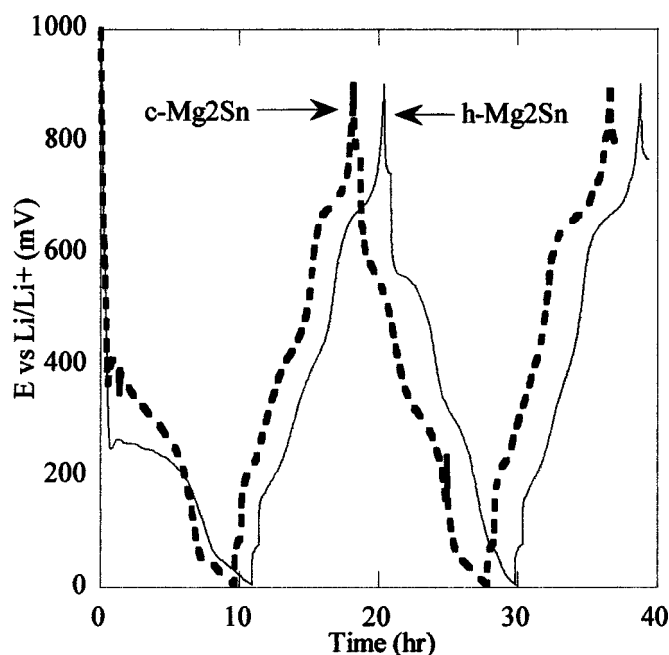


Figure 5. Galvanostatic results over 5-900 mV at C/10.

Since the exact nature of the metastable phase is still being debated, there are two observations from our milling experiments that may prove useful. First, we could not produce the metastable phase when milling with a large excess of magnesium. In this case, the elemental powder mixture had a stoichiometry of $\text{Mg}_{5.7}\text{Sn}$. Even after 50 h of milling, only Mg and c- Mg_2Sn were observed in the diffraction patterns. Second, we observed a complete transformation to the metastable phase by milling a pure c- Mg_2Sn starting material produced by hot isostatic pressing. By starting with a single phase powder, concerns about preferential cold welding between the elemental starting materials and the milling tools were avoided.

Galvanostatic cycling results.—Figure 5 shows electrode potential vs. time plots for electrodes prepared from separate samples of pure c- Mg_2Sn and h- Mg_2Sn materials. They were cycled over 5-900 mV vs. Li/Li^+ at 50 mA/g of active material (approximately C/10 rates). The c- Mg_2Sn electrode started to develop insertion capacity around 400 mV, but h- Mg_2Sn did not start to develop significant insertion capacity until 250 mV. After the first insertion, the remaining Li extraction and insertion profiles were very similar for both materials.

Cycling results for each cell are shown in Fig. 6. The c- Mg_2Sn electrode was cycled ten times, and the h- Mg_2Sn electrode was cycled twenty times. Both materials demonstrated promising performance in these preliminary cycling tests. They still retained reversible capacities of approximately 400 mAh/g in their final cycles.

In situ X-ray diffraction results.—The *in situ* XRD patterns and the corresponding voltage vs. time plot are shown for the first few hours for a h- Mg_2Sn cell in Fig. 7. This insertion proceeded until a cutoff potential of 5 mV was reached. During lithium insertion, the h- Mg_2Sn structure irreversibly converted to a cubic phase. This is consistent with the E vs. t plots in Fig. 5, which showed that the voltage profiles for c- Mg_2Sn and h- Mg_2Sn were similar after the first insertion. The only difference in the voltage profiles occurred during the first insertion, which can be attributed to the structural rearrangement required to convert the hexagonal phase to the cubic phase. Therefore, we would expect the two materials to cycle similarly with two caveats. First, major structural rearrangements can damage the mechanical integrity of the electrode, so the initial conversion from h- Mg_2Sn to the cubic structure could have detrimental

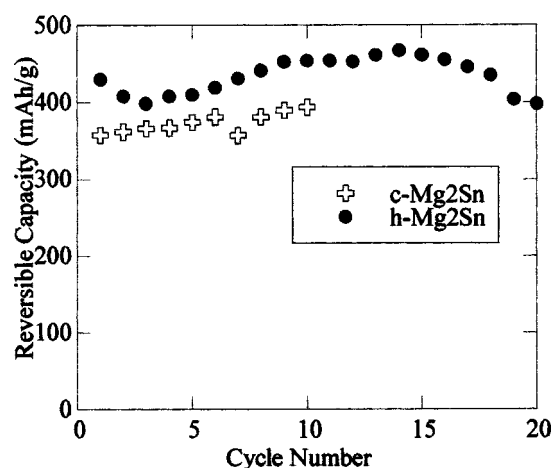


Figure 6. Cycling performance over 5-900 mV at C/10.

cycling effects. The preliminary cycling results in Fig. 6, however, show that the material starting as the hexagonal phase cycles as well as the material starting as the cubic phase. Second, the hexagonal phase is metallic, while pure c- Mg_2Sn has a semiconductor-type structure. Therefore, the h- Mg_2Sn electrodes should have a higher electrical conductivity during the initial stages of insertion before the conversion to the cubic phase is complete. However, the more difficult first insertion (as shown by the more negative activation potential) may negate any benefits that the originally more metallic structure may have provided.

In situ XRD patterns for a h- Mg_2Sn electrode are shown for a full cycle in Fig. 8. This cell was cycled over 15-900 mV. After the initial conversion of h- Mg_2Sn to a cubic phase, the diffraction patterns did not dramatically change throughout the rest of the cycle. Major new peaks did not develop, the existing peaks did not undergo noticeable peak shifts, and the intensities of the peaks did not substantially change.

Figure 9 shows the *in situ* XRD pattern for a h- Mg_2Sn cell after two complete cycles over 5-900 mV. The two strongest tin reflections are visible, which indicates that structural decomposition occurred when cycling over the wide 5-900 mV window.

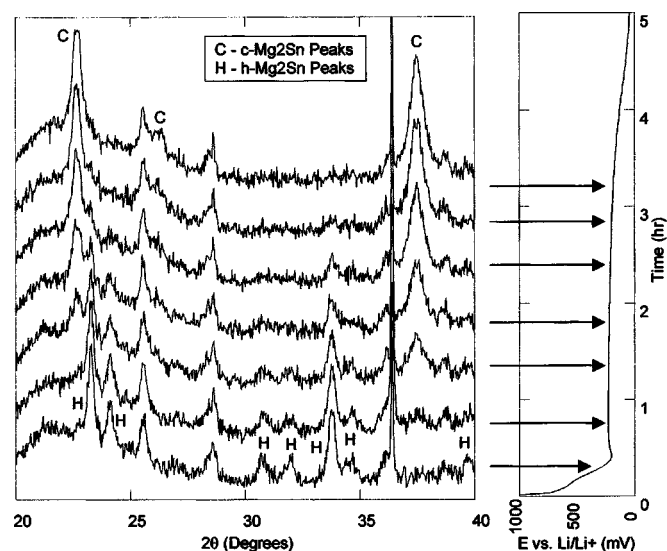


Figure 7. *In situ* XRD patterns for Li insertion to 5 mV at C/5 in h- Mg_2Sn .

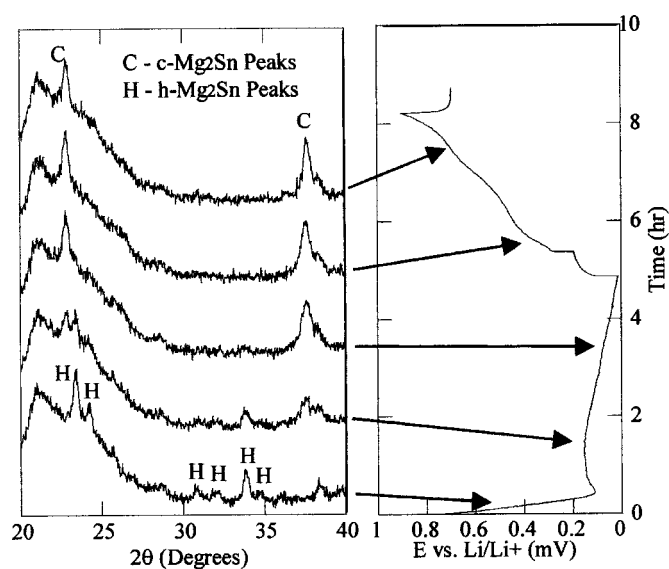


Figure 8. *In situ* XRD patterns for a cycle over 15-900 mV at C/5 for h-Mg₂Sn.

Reaction mechanism.—We propose that lithium insertion into Mg₂Sn produces a unique ternary phase, Li₂MgSn. This is similar to the mechanism that we have proposed for Li₂MgSi formation from Mg₂Si.⁵ The proposed electrochemical reaction is Mg₂Sn + 2Li⁺ + 2e⁻ ↔ Li₂MgSn + Mg. With Mg₂Si and Li₂MgSi, we could clearly see the coexisting peaks in the XRD patterns. However, it would be extremely difficult to observe the coexistence of c-Mg₂Sn (JCPDS number 07-0274) and Li₂MgSn (JCPDS number 42-1214) because these diffraction patterns essentially overlap. The phases have identical space groups (*Fm*₃*m*, number 225) and nearly identical lattice parameters (0.6764 nm for Li₂MgSn vs. 0.6763 nm for Mg₂Sn). Such small differences in peak positions would be below the resolution of our position-sensitive detector (0.029°) and would be difficult to detect even under optimal conditions.

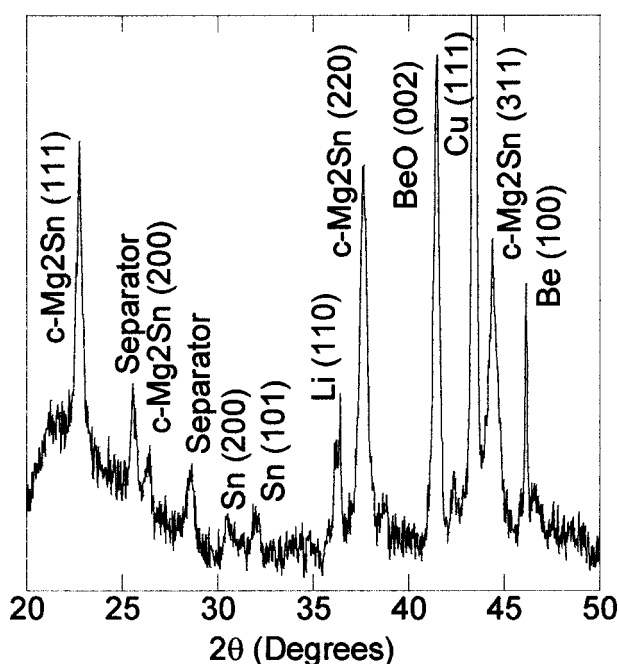


Figure 9. *In situ* XRD pattern after two 5-900 mV cycles for h-Mg₂Sn.

If Li₂MgSn was produced from Mg₂Sn, we would also expect to observe free Mg after formation of the unique ternary phase. Unfortunately, Mg is not an ideal element to study in the *in situ* XRD cell because Mg is a low Z element, has its strongest peak near a very strong Li peak from the lithium foil counter electrode, and would be expected to have broad peaks when formed by a solid-state discharge from the Mg₂Sn structure. In our work with Mg₂Si, we mainly used *ex situ* XRD to detect Mg. Fortunately, Kim *et al.* have high quality *ex situ* XRD patterns of Mg₂Sn after lithium insertion in the first cycle and after lithium removal in the first, second, third, fifth, and tenth cycles.¹⁷ Based on our mechanism, we would expect strong Mg peaks after lithium insertion into Mg₂Sn. The Mg peaks should disappear (or be greatly diminished if the reaction was not totally reversible) after lithium removal from the electrode. This is exactly what their *ex situ* XRD patterns show.¹⁷ A strong Mg peak is labeled after the first insertion, but it is barely detectable after completion of the first, second, and third cycles.

Conceding our inability to unambiguously identify Li₂MgSn in the diffraction patterns, we propose the following mechanism for lithium insertion:

1. Possible Li intercalation. This is difficult to confirm without clearly noticeable peak shifts, and we note that subtle peak shifts indicating intercalation could be below the 0.029° detection limit of our position-sensitive detector. Intercalation would follow parallels with the structurally similar material Mg₂Si, for which we observed shifting peaks.⁵ However, with the rapid onset of the formation of Li₂MgSn, the intercalation capacity would only make a small contribution to the total capacity.

2. Mg₂Sn + 2Li⁺ + 2e⁻ ↔ Li₂MgSn + Mg. The theoretical capacity for this reaction is 320 mAh/g. Any capacity beyond this limit would need to be provided by Li insertion into the magnesium from this reaction or by decomposition of the ternary phase to form binary Li-Sn phases. Both the cubic and hexagonal Mg₂Sn phases produce the cubic Li₂MgSn phase. The hexagonal to cubic transformation is irreversible. Lithium removal from Li₂MgSn will only produce c-Mg₂Sn.

3. Possible reversible reactions of Li with Mg produced in the previous step. This was observed for Li insertion in Mg₂Si.⁵ As long as the cathodic potential limit is low enough, Li should be able to form a solid solution with the magnesium product from the previous step.

4. Conversion of the ternary phase into binary lithium compounds to permit Li-Sn reactions. This is confirmed by very weak tin peaks in our diffraction patterns after a few cycles and by the Kim *et al.* differential capacity plots that show strong peaks characteristic of Li-Sn reactions that develop during cycling.

In the Kim *et al.* study, the differential capacity plots for the first cycle do not have peaks at the same potentials as pure tin electrodes.¹⁷ Since it is unlikely that 2.5-3 Li could be inserted without major structural changes in an intercalation reaction, we believe that the formation of a ternary phase such as Li₂MgSn more adequately justifies the large lithium capacities. Due to the near overlaps of the indexed patterns for c-Mg₂Sn and Li₂MgSn, we would not expect to see major changes in the diffraction patterns after the initial conversion of the hexagonal phase to the cubic phase. Also, the Kim *et al.* *ex situ* XRD patterns, which show strong magnesium peaks after lithium insertion but weak magnesium peaks after lithium removal, are consistent with the formation of Li₂MgSn.¹⁷ Incomplete reversibility of this reaction should ultimately lead to Mg accumulation during cycling. Further lithium insertion apparently decomposes Li₂MgSn to allow for the formation of Li-Sn phases.

Conclusions

The preliminary cycling results have shown that Mg₂Sn is an intermetallic worthy of more investigation as a negative electrode material. The results are promising because high reversible capaci-

ties of approximately 400 mAh/g were obtained for 20 cycles without rapid capacity fading. Optimization of the cycling conditions (*e.g.*, electrolyte composition, voltage cutoff limits, current density, and operating temperature) may lead to further improvements.

The formation of the metastable phase during milling is an interesting phenomenon, but our cycling results indicate that it does not affect the material's electrochemical performance. The metastable, hexagonal structure is irreversibly destroyed during the first lithium insertion.

As with the formation of Li_2MgSi during lithium insertion into Mg_2Si , it is possible that lithium insertion into Mg_2Sn produces Li_2MgSn . The formation of this phase would satisfactorily describe the XRD results. The nearly identical XRD patterns for Mg_2Sn and Li_2MgSn and the observation of Mg peaks when fully lithiated support this proposed mechanism. The stable cycling behavior could be attributed to the similarities between the lithiated and unlithiated structures.

Further research into magnesium stannide's cycling behavior and reaction mechanisms is warranted. Directly synthesizing the Li_2MgSn phase for characterization and mechanistic work would be useful. Since the indexed patterns for Mg_2Sn and Li_2MgSn are so similar, other characterization techniques should be employed to complement the XRD work.

Acknowledgments

This work was supported by the Assistant Secretary for Energy Efficiency and Renewable Energy, Office of Transportation Technologies, Office of Advanced Automotive Technologies of the U.S. Department of Energy under contract no. DE-AC01-76SF00098. We

thank Karl Gross and Scott Spangler for the use of their X-ray facilities and for their expertise.

Sandia National Laboratories assisted in meeting the publication costs of this article.

References

1. K. C. Hewitt, L. Y. Beaulieu, and J. R. Dahn, *J. Electrochem. Soc.*, **148**, A402 (2001).
2. J. T. Vaughey, J. Ohara, and M. M. Thackeray, *Electrochem. Solid-State Lett.*, **3**, 13 (2000).
3. D. Larcher, L. Y. Beaulieu, D. D. MacNeil, and J. R. Dahn, *J. Electrochem. Soc.*, **147**, 1658 (2000).
4. K. D. Kepler, J. T. Vaughey, and M. M. Thackeray, *J. Power Sources*, **82**, 383 (1999).
5. G. A. Roberts, E. J. Cairns, and J. A. Reimer; In preparation.
6. G. A. Roberts, E. J. Cairns, and J. A. Reimer, *J. Power Sources*, **110**, 424 (2002).
7. S. W. Song, K. A. Striebel, R. P. Reade, G. A. Roberts, and E. J. Cairns, *J. Electrochem. Soc.*, **150**, A121 (2003).
8. H. Kim, J. Choi, H. Sohn, and T. Kang, *J. Electrochem. Soc.*, **146**, 4401 (1999).
9. T. Moriga, K. Watanabe, D. Tsuji, S. Massaki, and I. Nakabayashi, *J. Solid State Chem.*, **153**, 386 (2000).
10. P. Cannon and E. Conlin, *Science (Washington, DC, U.S.)*, **145**, 487 (1964).
11. T. I. Dyuzheva, N. A. Bendeliani, L. N. Dzhavadov, T. N. Kolobyanina, and N. A. Nikolae, *J. Alloys Compd.*, **223**, 74 (1995).
12. K. J. Range, G. H. Grosch, and M. Andratschke, *J. Alloys Compd.*, **244**, 170 (1996).
13. J. Schilz, M. Riffel, K. Pixius, and H. J. Meyer, *Powder Technol.*, **105**, 149 (1999).
14. C. R. Clark, C. Wright, C. Suryanarayana, E. G. Baburaj, and F. H. Froes, *Mater. Lett.*, **33**, 71 (1997).
15. G. Urretavizcaya and G. O. Meyer, *J. Alloys Compd.*, **339**, 211 (2002).
16. H. Sakaguchi, H. Maeta, M. Kubota, H. Honda, and T. Esaka, *Electrochemistry (Tokyo, Jpn.)*, **68**, 632 (2000).
17. H. Kim, Y. J. Kim, D. G. Kim, H. J. Sohn, and T. Kang, *Solid State Ionics*, **144**, 41 (2001).
18. C. Suryanarayana, *Prog. Mater. Sci.*, **46**, 1 (2001).